photonics

Article

A Multi-Layer Erbium-Doped Air-Hole-Assisted Few-Mode Fiber with Ultra-Low Differential Modal Gain

Zhiqi Li [1,2], Li Pei [1,2], Jingjing Zheng [1,2,*], Jianshuai Wang [1,2], Wenxuan Xu [1,2], Tigang Ning [1,2] and Jing Li [1,2]

1 Institute of Lightwave Technology, Beijing Jiaotong University, Beijing 100044, China; 19111027@bjtu.edu.cn (Z.L.); lipei@bjtu.edu.cn (L.P.); wangjsh@bjtu.edu.cn (J.W.); 19120022@bjtu.edu.cn (W.X.); tgning@bjtu.edu.cn (T.N.); lijing@bjtu.edu.cn (J.L.)
2 Key Laboratory of All Optical Network and Advanced Telecommunication Network of Ministry of Education, Beijing Jiaotong University, Beijing 100044, China
* Correspondence: jjzheng@bjtu.edu.cn

Abstract: The air-hole assisted few-mode fiber (AH-FMF) enables modal intensity balance and offers a profound prospect in gain equalization with the combination of adaptive ion doping. In this paper, we proposed an AH-FM-EDF with a multi-layered erbium doping profile. In AH-FM-EDF, due to the central air hole, only the first radial order modes (LP_{01}, LP_{11}, LP_{21}, and LP_{31}) are supported, and all the modes are confined in the same high refractive index core region. The differential modal gain (DMG) is highly reduced by optimizing the erbium doping proportion in each layer. Compared with uniform doping, the DMG is reduced from 4 dB to 0.14 dB as triple-layer doping is deployed. Additionally, the proposed erbium-doped fiber performs well in gain flattening and fabrication tolerance over the whole C-band.

Keywords: mode division multiplexing (MDM); air-hole assisted; few-mode erbium-doped fiber amplifier (FM-EDFA); gain equalization

Citation: Li, Z.; Pei, L.; Zheng, J.; Wang, J.; Xu, W.; Ning, T.; Li, J. A Multi-Layer Erbium-Doped Air-Hole-Assisted Few-Mode Fiber with Ultra-Low Differential Modal Gain. *Photonics* **2022**, *9*, 305. https://doi.org/10.3390/photonics9050305

Received: 15 April 2022
Accepted: 28 April 2022
Published: 29 April 2022

1. Introduction

Mode-division multiplexing (MDM) transmission over few-mode fibers (FMF) is a promising candidate to overcome the capacity limitation of single-mode fibers (SMF) [1–4]. It utilizes multiple modes on a single core at the same time, contributing to an efficient capacity expansion. The few-mode erbium-doped fiber amplifiers (FM-EDFAs) are required for long-haul transmission signal amplification [5–7]. Due to the different modal loss and mode field distribution, a large differential modal gain (DMG) is probably aroused after amplification. The power discrepancy between signals hinders the stability of the MDM system and the bit error rate may be unacceptable after long-haul transmission or multi-stage amplification. Therefore, researchers try to obtain the gain equalization in FM-EDFA by refractive index (RI) [8–10] or doping profile design [8,11–13] of the FM-EDF as well as the pump optimization [1,14–16].

In the FM-EDFAs, a large DMG may arise due to the obvious different modal profile between the convergent Gaussian-like LP_{01} and divergent LP_{mn} ($m \geq 0$, $n > 1$) modes in the step-index FM-EDF. In this case, FM-EDFs were designed to balance the modal patterns by introducing a dip in the fiber center [17]. Yung first demonstrated an FM-EDFA by using an FM-EDF with a tailored central dip [18], where the DMG is lowered by 2 dB more than the traditional step-index fiber. With the depending dip, the ring-core fiber (RCFs) is formed when the RI of the central region is equal to the clad. In RCF, a high- RI ring core is sandwiched between the two low- RI regions. RCF has been proved to have much potential in gain equalization. In 2015, a 2-LP ring-core FM-EDF is fabricated and a small DMG (~1 dB) is realized [19]. With the aim of increasing the supporting mode number, a trench-assisted five-mode ring-core erbium-doped fiber amplifier was proposed with a DMG of ~1 dB, while the gain is only 10 dB [20]. However, the RCF may not be satisfactory in mode modification due to its poor fabrication tolerance. Usually, in RCF, both the model number and sequence are sensitive to the thickness of the central dip and the RI difference between the core and cladding.

The air-hole-assisted few-mode fiber (AH-FMF) has a higher RI depression in the central than the RCF, thus enabling a stronger capability in modal intensity modification [21–24]. In the air-hole-assisted few-mode fiber, the high-refractive-index annular core (HRI-AC) is sandwiched between the air hole and the cladding. Due to the weak light confinement ability of the air hole, all the modes tend to be confined in the high-refractive-index annular core. It benefits for balancing the value of the overlap integral factors between different signal and pump mode groups, contributing to a low DMG. For instance, in a traditional step-index FMF (SI-FMF), the LP_{01} mode distributes as a convergence Gaussian shape and its modal gain is much higher than other divergence high-order modes [8,16]. While in the air-hole-assisted few-mode fiber, the LP_{01} mode is restricted into the annual core region and the modal intensity is similar to other high-order modes. This contributes to the semblable overlap integral factors and benefits the FM-EDFA for gain equalization. In addition, the central air hole changes the mode cutoff condition. With the introduction of the central air hole, the fiber only supports single-radial-order modes (i.e., LP_{m1} modes where m is an integer), enlarging the effective RI between modes, which significantly reduces the modal crosstalk and coupling. In the terms of modal amplification, all of the guided modes possess similar modal intensities. On that basis of appropriate pump selection and an adaptive erbium-doping profile, the air-hole-assisted few-mode fiber is bound to provide an excellent ability in gain equalization.

In 2015, Kang et al. proposed an air-core erbium-doped fiber (AC-EDF). It theoretically analyzed the fiber performance under core pumping and cladding pumping conditions [15]. The relationship between DMG and pump mode selection was investigated. It is verified that the cladding pumping is independent to the pump mode selection and it is promising in constructing a stable all-fiber scheme. Compared with the uniform ion doping, the DMG is reduced to lower than 2 dB with a multi-layered ion profile under cladding pumping. Then, Jung et al. proposed a cladding-pumped air-hole-assisted erbium-doped fiber amplifier (AH-EDFA), which further verified the influence of cladding pumping on the amplifier [25]. In the analysis, a 4 m length of air-hole-assisted erbium-doped fiber (AH-EDF) and the 976 nm multimode pump was selected. A peak gain of 15.7 dB is obtained at 1565 nm, and in the wavelength range of 1555 nm to 1590 nm, the gain remains higher than 10 dB. It only focuses on the specific output signal power, while the DMG is not further discussed.

From the former research, it can be found that when the central air hole is introduced to the core, the high RI difference between the air hole and silica core can effectively adjust the mode field distribution and restrict them into the ring-shaped core. It can initially reduce the differences between mode field distribution, thereby achieving similar gains and low DMG combined with the doping design. In this paper, we proposed an air-hole-assisted few-mode erbium-doped fiber (AH-FM-EDF). The mode field distribution of different guided modes, especially the gaussian distribution LP_{01} mode, can be adjusted and is beneficial to gain equalization. With multi-layer erbium-ion doping in the ring-shaped core based on the particle swarm optimization (PSO) algorithm, the gain of ~20 dB is obtained and the DMG is reduced from 4 dB (uniform doping) to 0.14 dB (triple-layer doping). It performs well in gain-flattening and fabrication tolerance over the whole C-band.

2. Theory and Model

The amplification of the FM-EDFA is based on a quasi-three-level erbium-ion system [26] and two groups of differential equations are used in the simulation: rate and propagation equations [8]. N_0 is the dopant density of the erbium-doped fiber (EDF), and τ is the spontaneous emission lifetime of the erbium ions. As the erbium ions in the excited state is negligible, the erbium-ion system under 980 nm pump can be regarded as a two-level system. The populations in upper and lower energy levels at the position (r, φ, z) are $N_1(r, \varphi, z)$ and $N_2(r, \varphi, z)$, given by

$$N_1(r,\varphi,z)=\frac{\left[\frac{1}{\tau}+\frac{1}{hv_s}\sum_{i=1}^{m_s}[P_{ASE,i}(z)+P_{s,i}(z)]\sigma_{es}\Gamma_{s,i}(r,\varphi)\right]N_0(r,\varphi)}{\left[\frac{1}{hv_s}\sum_{i=1}^{m_s}[P_{ASE,i}(z)+P_{s,i}(z)](\sigma_{es}+\sigma_{as})\Gamma_{s,i}(r,\varphi)+\frac{1}{\tau}+\frac{1}{hv_p}\sum_{j=1}^{m_p}P_{p,j}(z)\sigma_{ap}\Gamma_{p,j}(r,\varphi)\right]}, \tag{1}$$

$$N_2(r,\varphi,z)=N_0(r,\varphi,z)-N_1(r,\varphi,z), \tag{2}$$

where $\Gamma_{s,i}(r,\varphi)$ and $\Gamma_{p,j}(r,\varphi)$ are the normalized intensity patterns of the *i-th* signal mode and *j-th* pump mode of the active fiber, h is Planck constant, σ_{as} and σ_{ap} are the absorption cross-section areas at signal and pump wavelengths, σ_{es} and σ_{ep} are the emission cross-section areas, m_s/m_p and v_s/v_p are the total number of guided modes and optical frequency at λ_s and λ_p, respectively.

The power in signal mode i ($P_{s,i}$), the amplified spontaneous emission (ASE) power in signal mode i ($P_{ASE,i}$), and pump power in mode j ($P_{p,j}$) evolve as below, where Δv is the equivalent amplifying bandwidth and a stands for the radius of uniform doping region.

$$\frac{dP_{s,i}}{dz}=P_{s,i}\int_0^{2\pi}\int_0^{a}\Gamma_{s,i}(r,\varphi)[N_2(r,\varphi,z)\sigma_{es}-N_1(r,\varphi,z)\sigma_{as}]rdrd\varphi, \tag{3}$$

$$\frac{dP_{ASE,i}}{dz}=P_{ASE,i}\int_0^{2\pi}\int_0^{a}\left\{\Gamma_{s,i}(r,\varphi)\,[N_2(r,\varphi,z)\sigma_{es}-N_1(r,\varphi,z)\sigma_{as}]+2\sigma_{es}hv_s\Delta vN_2(r,\varphi,z)\Gamma_{s,i}(r,\varphi)\right\}rdrd\varphi, \tag{4}$$

$$\frac{dP_{p,j}}{dz}=-P_{p,j}\int_0^{2\pi}\int_0^{a}\Gamma_{p.j}(r,\varphi)N_1(r,\varphi,z)\sigma_{ap}rdrd\varphi, \tag{5}$$

The gain of the signal and the DMG of the amplifier is defined as

$$Gain(dB)=10\log_{10}\frac{P_{s,i}(z=l)}{P_{s,i}(z=0)}, \tag{6}$$

$$DMG(dB)=\max(Gain)-\min(Gain). \tag{7}$$

From the former equations, the modal gain of different modes in an FM-EDFA is affected by $\Gamma_{s,i}(r,\varphi)$, $\Gamma_{p,j}(r,\varphi)$ and $n_0(r,\varphi)$, which can be expressed by the overlap integral, where $n_0(r,\varphi)$ is the doping concentration of erbium-ion in the core.

$$\eta_{s,i}^{p,j}=\int_0^{2\pi}\int_0^{a}\Gamma_{s,i}(r,\varphi)\Gamma_{p,j}(r,\varphi)n_0(r,\varphi)rdrd\varphi, \tag{8}$$

Due to the pump mode selection independence, we analyze the characteristics of FM-EDFA under cladding pumping condition. Thus, $\Gamma_{p,j}(r,\varphi)$ is a constant, and the overlap integral factors are only determined by the normalized intensity of the signal modes and the doping profile.

The normalized intensity of different guided modes can be adjusted according to the introduction of the central air hole in the AH-FM-EDF. However, since the differences still exist only considering the RI, multi-layer doping designs are taken into account to further balance the overlap integral factors, which have different concentrations in different regions. The design of the erbium-ion doping profile is usually non-coincident with the fiber RI profile, as it can further eliminate the gain differences. The combination of the refractive index and doping profile design can effectively reduce the DMG between different guided modes and is conducive to the gain equalization of the FM-EDFA.

Several intelligent methods have been proposed for the EDF design in both the refractive index and doping profile, including the genetic algorithm (GA) [27,28], particle swarm optimization (PSO) [29] and gradient descent optimization (GDO) [30]. In this paper, the erbium-ion doping profile of the proposed AH-FM-EDF is optimized under PSO, and the optimal doping radius and the concentrations were obtained under double- and triple layer doping design, which can balance the overlap integral factors of different pump-signal mode groups and is beneficial to the gain equalization.

The proposed AH-FM-EDF is composed of a central air hole, an HRI-AC, and cladding, which is illustrated in Figure 1a. With the central air hole, the modal intensity profile is different from the traditional step-index fiber, as shown in Figure 1b, where a_{air} = 2 μm, a_{co} = 9 μm, n_{co} = 1.452, and n_{cl} = 1.444. The central intensity of the LP_{01} mode is strongly depressed. All the modes are confined in the HRI-AC and similar normalized intensities can be obtained. Differing from the step-index fiber, the LP_{02} is cut off before the LP_{31}. The first radial order modes (LP_{01}, LP_{11}, LP_{21}, and LP_{31}) are supported in the AH-FM-EDF. The effective RI (ERI) of the signal modes in the C-band is illustrated in Figure 1c. As shown in the figure, the minimal value of the ERI difference is higher than 1×10^{-3} over the whole C-band. The normalized intensities and ERI of different guided modes have been carried out using COMSOL Multiphysics software. It is verified that the proposed AH-FM-EDF has excellent modal isolation and it relatively avoids the mode coupling in signal amplification.

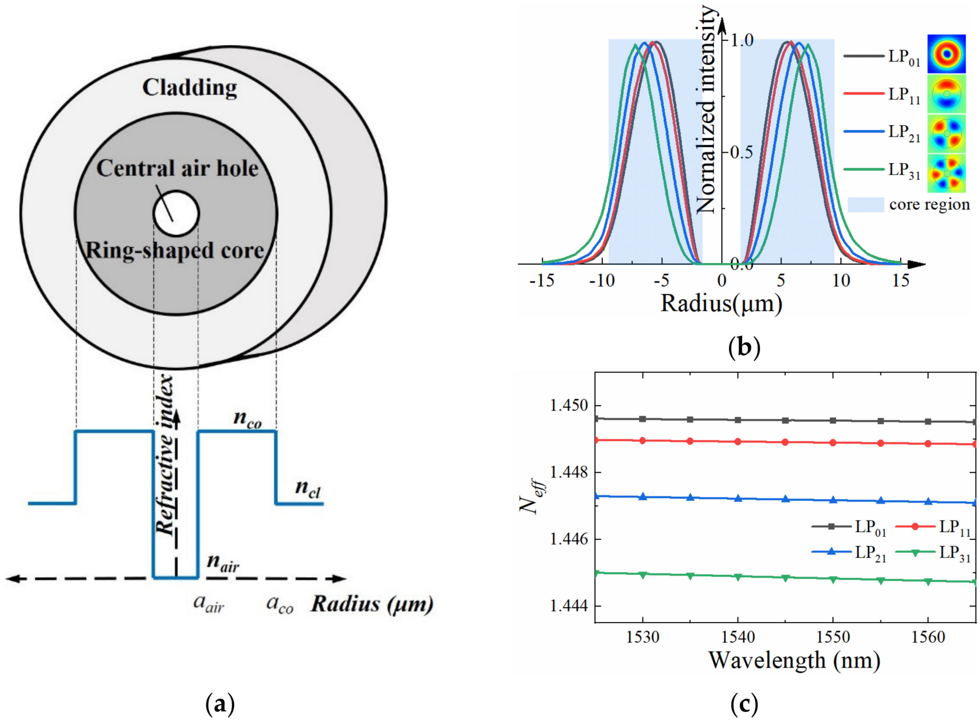

Figure 1. (**a**) Schematic diagram and the refractive index distribution of the AH-FM-EDF; (**b**) Normalized intensities and (**c**) effective refractive indices of the guide modes.

3. Results and Discussions

Besides the RI of the fiber, the DMG correlates with the erbium doping profile. Normally, more accurate amplification can be obtained between different modes when the number of doping-layers increases. It is worth mentioning that the PSO algorithm can achieve the concentration optimization under any number of layers. Considering the fabrication in practice, we analyzed three types of dopants profiles in the following section, including single layer (uniform doping), double-layer, and triple-layer doping. The three types of doping profiles are illustrated in Figure 2. The doping boundaries are set as r_1, r_2, and r_3. The corresponding doping concentration from the inside out is N_1, N_2, and N_3. In the simulation, the degenerate states of the signal mode are not considered. Each signal input power is set as −10 dBm. The pump power is set as 3 W. The PSO algorithm is applied to determine the doping concentration and boundaries.

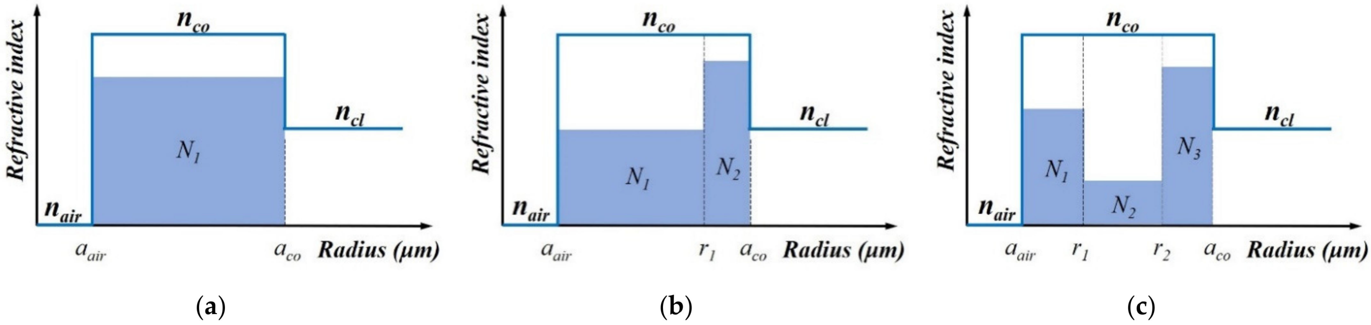

Figure 2. Different doping profile. (**a**) uniform doping; (**b**) double-layer doping; (**c**) triple-layer doping.

In the first uniform doping profile, the erbium ion concentration is 4.4×10^{25} m^{-3}. Then in the double and triple-layer cases, the doping radius and concentration are iteratively optimized by the PSO algorithm. The results are shown as below.

$$\text{Double}-\text{layer:}\begin{cases} N_1 = 2.5 \times 10^{25}\ \text{m}^{-3}, 2 \le r \le 7.72 \\ \\ N_2 = 6.1 \times 10^{25}\ \text{m}^{-3}, 7.72 < r \le 9 \end{cases}$$

$$\text{Triple}-\text{layer}: \begin{cases} N_1 = 4.84 \times 10^{25}\ \text{m}^{-3}, 2 \le r \le 4.5 \\ N_2 = 1.13 \times 10^{25}\ \text{m}^{-3}, 4.5 < r \le 7.36 \\ N_3 = 6.39 \times 10^{25}\ \text{m}^{-3}, 7.36 < r \le 9 \end{cases}$$

The gains and DMG of the three doping cases are shown in Figure 3, where Figure 3a–c corresponds to the gain characteristics under uniform-, double-layer, and triple-layer doping, and Figure 3d illustrates the DMG results. It can be found from Figure 3a that at uniform doping, there is a big difference in gains and the DMG is more than 4 dB (LP_{01} = 24.79 dB, LP_{11} = 23.45 dB, LP_{21} = 22.39 dB, LP_{31} = 20.12 dB) at the fiber length of 1 m. Then, with the PSO algorithm, the signal gains in the double- and triple-layer cases are illustrated in Figure 3b,c. Under the same conditions, the gains are all higher than 20 dB in double- and triple-layer doping cases. Comparing the DMG results under different doping cases as shown in Figure 3d, the DMG of double-layer doping is effectively reduced to 0.55 dB and a DMG of 0.14 dB is further obtained in the triple-layer doping cases. Actually, the simulation results under four-layer doping cases have also been carried out. However, the DMG cannot be further reduced through the increase in the number of doping layers. The triple-layer doping case is considered the optimal solution for the proposed AH-FM-EDF.

Due to the low DMG of 0.14 dB at the wavelength of 1550 nm, the following discussion is implemented in the triple-layer doping cases. The gain characteristics over the whole C-band is illustrated in Figure 4. All the signal gains are higher than 19 dB. In the wavelength range of 1530–1550 nm, the DMG keeps lower than 0.15 dB. At the wavelength 1525 and 1565 nm, the DMG are 0.21 dB and 0.26 dB, respectively. Consequently, at each wavelength, the DMG is lower than 0.3 dB. Moreover, due to the similar signal gains, there is an excellent gain flatness within 1 dB over the C-band.

As we all know, it is impossible to maintain a stable gain value at any signal input power level for an FM-EDFA. It provides more gains to the small signals and less to the large ones, which is called the gain saturation effect [31]. The maximum output capability of the FM-EDFA is characterized by the saturated signal output power. It is defined as the corresponding output power when the saturated gain of each mode drops by 3 dB. The relationship between the gains of the proposed AH-FM-EDFA and the signal input power is investigated and simulated in the case of triple-layer doping design, as shown in Figure 5. From the figure, it can be seen that when the signal input power varies from −40 dBm to 5 dBm, the DMG is relatively low (<0.35 dB). The gain equalization characteristics perform well and the saturated signal input power of different modes can be regarded as equal, about −17.7 dBm. The saturated output power of the AH-FM-EDFA can reach 20 mW, which means the maximum output capability of the amplifier.

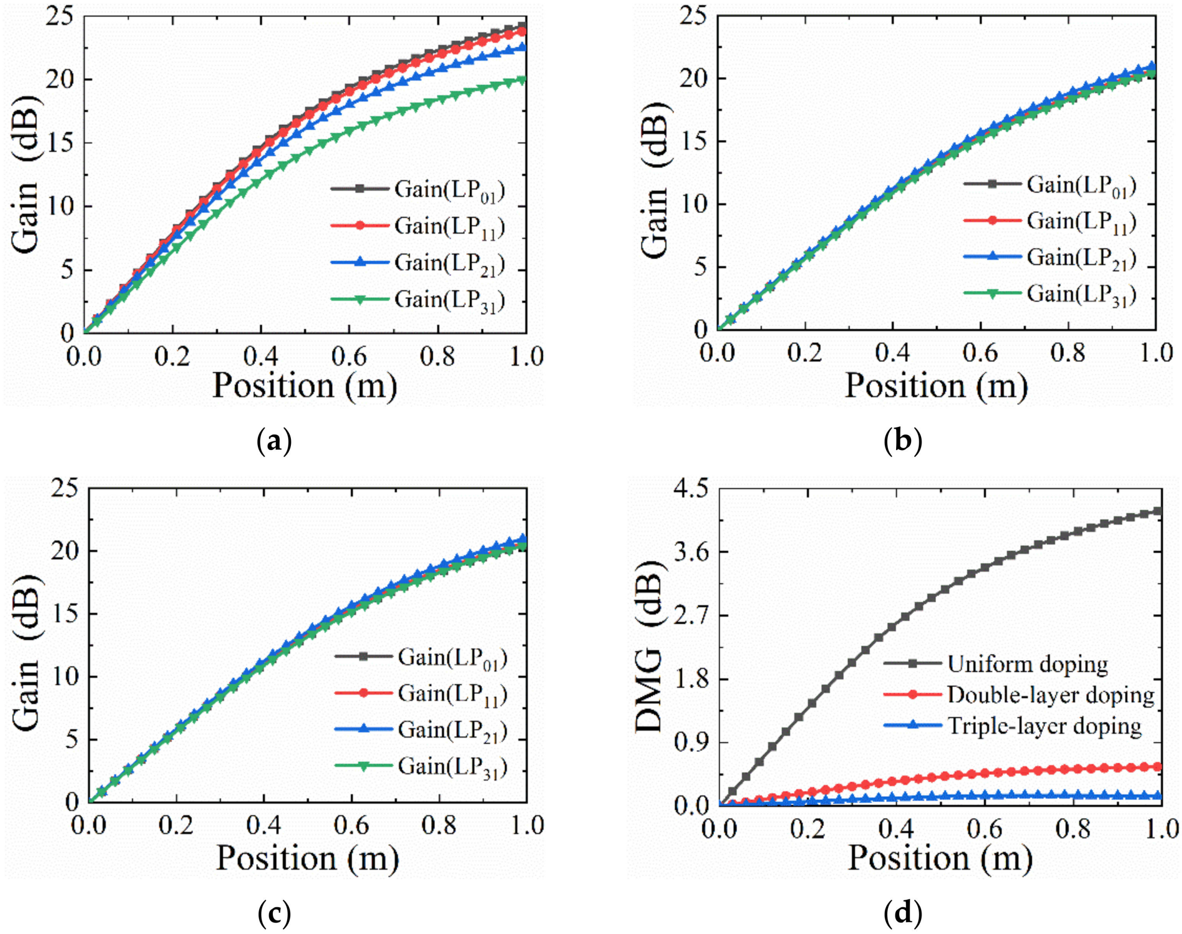

Figure 3. Gain characteristics under (**a**) uniform-, (**b**) double-layer, and (**c**) triple-layer doping design. (**d**) DMG versus fiber length.

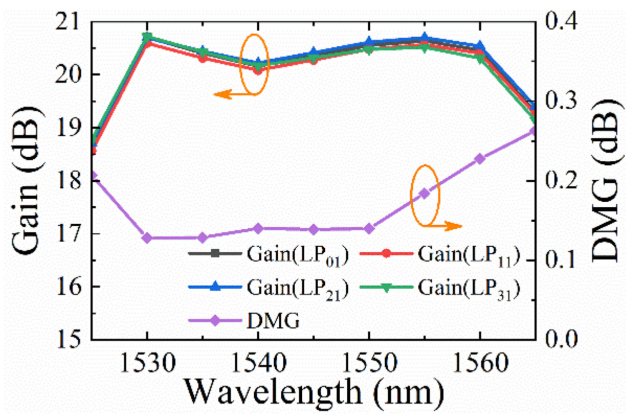

Figure 4. Gains and DMG versus signal wavelength.

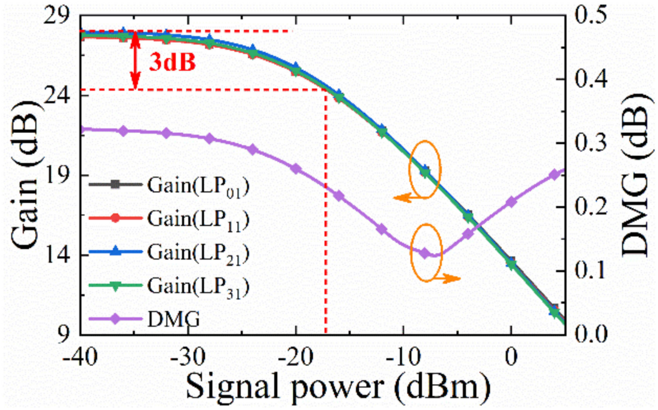

Figure 5. Gain saturation characteristic.

Since the gain characteristics of the AH-FM-EDF are optimized under the length of 1 m and 3000 mW pump power, the gains and DMGs under different fiber length and pump power are further analyzed, as shown in Figure 6. The gain and DMG are illustrated in Figure 6a, with the length varying from 0.5 m to 3 m. As the fiber length is more than 0.9 m, signal gains are higher than 20 dB. In range of 1 m to 1.8 m for the fiber length, the DMG remains lower than 0.3 dB. Figure 6b illustrates the gains and DMG as the pump power varies. It can be seen that gains of different guided modes are higher than 20 dB and the pump power is higher than 3000 mW, and meanwhile the DMG is stabilized below 0.2 dB. Although the optimization of the doping profile is considered in the case of 3000 mW cladding pumping and 1 m length of fiber, the proposed AH-FM-EDF still performs well in gain equalization under different fiber length and pump power.

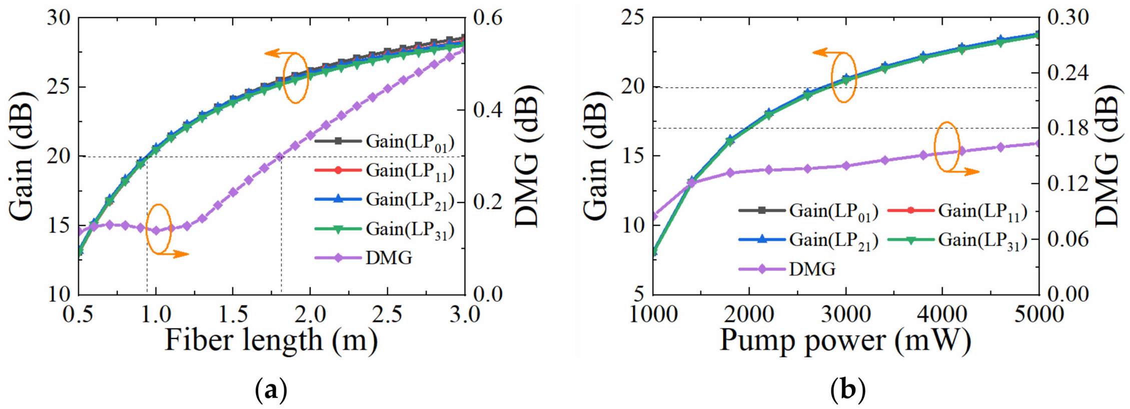

Figure 6. Gains and DMG versus (**a**) fiber length (under 3000 mW pump power) and (**b**) pump power (under 1 m length of AH-FM-EDF).

Furthermore, as the inevitable imperfections always occur in practical manufacturing, the influences on the fabrication tolerance characteristics of the proposed AH-FM-EDF are further explored. However, due to the fiber fabrication, the RI and radius control have been relatively mature. Herein, the discussion about the fabrication tolerance is focused on the central air hole and the doping concentration deviation. The fabrication tolerance on the radius of the central air hole is illustrated in Figure 7. When the air hole radius is under ±5% and ±10% offset conditions, the DMG of the AH-FM-EDFA remains lower than 0.3 dB over the whole C-band and the minimum gain of the amplifier can reach 20 dB at 1550 nm signal wavelength.

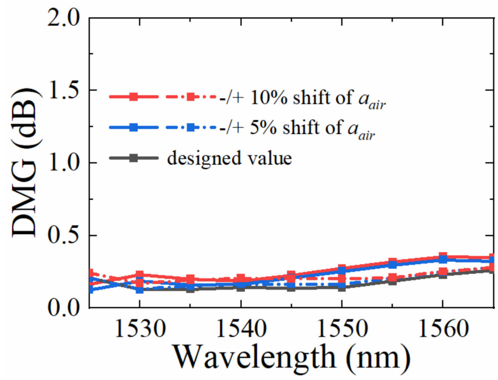

Figure 7. DMG versus wavelength under the shift of central air hole.

The doping concentration variation is analyzed with ±5% and ±10% offsets. The results are shown in Figure 8, and Figure 8a–c correspond to N_1 to N_3. From the figure, it can be seen that when the doping concentration offset occurs in N_1 and N_3, the maximum DMG of the amplifier is up to 0.8 dB (under the deviation of ±10%). And when the doping concentration happens to N_2, low DMG (<0.4 dB) can be realized. Within the ±10% fabrication tolerance on doping concentrations, DMGs over the whole C-band can be controlled within 0.8 dB. Thus, even if the fabrication error occurs in the doping process, the gain equalization characteristics still perform well, which is beneficial to the actual manufacturing.

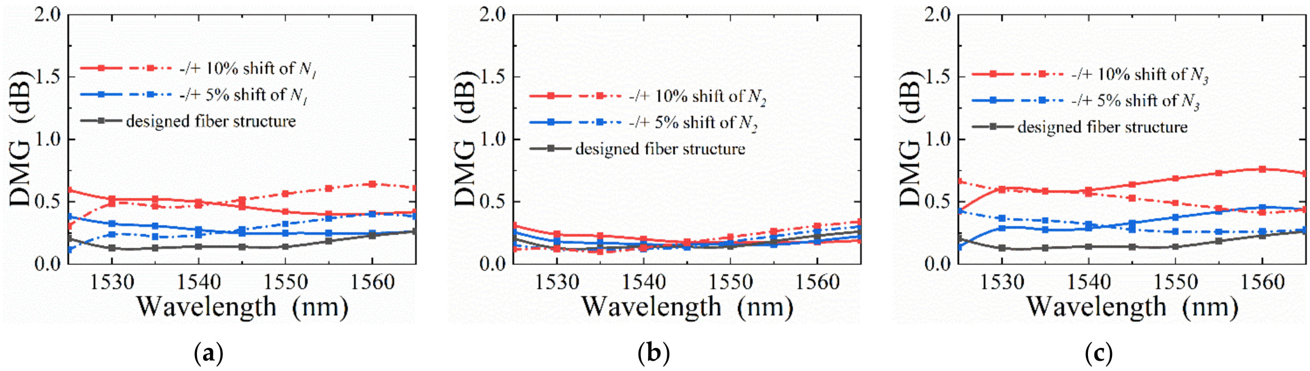

Figure 8. DMG versus wavelength under the shift of doping concentration of each layer, where (**a–c**) corresponds to the N_1 to N_3.

For the active air-hole fiber, the production of the AH-EDF was realized by the modified chemical vapor deposition (MCVD) process [25], and the femtosecond laser can be used to form the void in the fiber core [24]. Considering the development of the layer-doped technology, we believe that the fabrication of the multi-layer doped AH-FM-EDF can be realized.

4. Conclusions

In conclusion, a multi-layer-doped AH-FM-EDF is proposed and the PSO is applied to the doping concentration adjustment for low DMG. The adjustment of the modal intensity distribution to different guided modes is achieved with the introduction of the central air hole. A higher degree of overlap of integral factors can be obtained. According to the multi-layer doping design of the ring-shaped core, the DMG of the AH-FM-EDFA can be effectively reduced from 4 dB (uniform doping) to 0.14 dB (triple-layer doping) with gains of more than 20 dB. The fiber has a good gain-flattening characteristic in the whole C-band. From the simulations, the fiber we proposed has a good fabrication tolerance to the variation of doping concentration and air hole radius. Low DMG (<0.8 dB) can be realized under the ±10% offsets of doping concentration and air hole radius.

Author Contributions: Conceptualization, Z.L. and L.P.; methodology, J.W.; software, Z.L. and W.X.; validation, Z.L. and W.X.; formal analysis, Z.L. and J.Z.; investigation, T.N. and J.L.; resources, T.N. and J.L.; data curation, Z.L.; writing—original draft preparation, Z.L.; writing—review and editing, Z.L. and J.W.; visualization, Z.L.; supervision, L.P. and J.Z.; project administration, L.P.; funding acquisition, L.P. All authors have read and agreed to the published version of the manuscript.

Funding: This work was funded by the National Key R & D Program of China (2018YFB1801003), the National Natural Science Foundation of China (61827817, 62005012) and the Fundamental Research Funds for the Central Universities (2021YJS010).

Institutional Review Board Statement: Not applicable.

Informed Consent Statement: Not applicable.

Data Availability Statement: Not applicable.

Conflicts of Interest: The authors declare that they have no conflict of interest.

References

1. Wyrowski, F.; Sheridan, J.T.; Tervo, J.; Meuret, Y.; Herbster, A.; Romero, M.A. On the design of few-mode Er-doped fiber amplifiers for space-division multiplexing optical communications systems. In Proceedings of the Optical Modelling and Design III, Brussels, Belgium, 15–17 April 2014.
2. Desurvire, E.B. Capacity Demand and Technology Challenges for Lightwave Systems in the Next Two Decades. *J. Lightwave Technol.* **2006**, *24*, 4697–4710. [CrossRef]
3. Tkach, R.W. Scaling optical communications for the next decade and beyond. *Bell Labs Tech. J.* **2010**, *14*, 3–9. [CrossRef]
4. Essiambre, R.J.; Mecozzi, A. Capacity Limits in Single-Mode Fiber and Scaling for Spatial Multiplexing. In Proceedings of the Optical Fiber Communication Conference 2012, Los Angeles, CA, USA, 4–8 March 2012; p. OW3D.1.
5. Ezra Ip, N.B.; Huang, Y.K.; Mateo, E.; Yaman, F.; Li, M.J.; Bickham, S.; Ten, S.; Liñares, J.; Montero, C.; Moreno, V.; et al. 88 × 3 × 112-Gb/s WDM transmission over 50 km of three-mode fiber with inline few-mode fiber amplifier. In Proceedings of European Conference and Exposition on Optical Communications 2011, Geneva Switzerland, 18–22 September 2011; p. Th.13.C.12.
6. Sleiffer, V.A.J.M.; Veljanovski, V.; van Uden, R.G.H.; Kuschnerov, M.; Kang, Q.; Grüner-Nielsen, L.; Sun, Y.; Richardson, D.J.; Alam, S.; Poletti, F.; et al. 73.7 Tb/s (96 × 3 × 256-Gb/s) mode-division-multiplexed DP-16QAM transmission with inline MM-EDFA. In Proceedings of the European Conference and Exhibition on Optical Communication 2012, Amsterdam, The Netherlands, 16–20 September 2012; p. Th.3.C.4.
7. Sleiffer, V.A.; Leoni, P.; Jung, Y.; Surof, J.; Kuschnerov, M.; Veljanovski, V.; Alam, S.U.; Richardson, D.J.; Gruner-Nielsen, L.; Sun, Y.; et al. 20 × 960-Gb/s Space-division-multiplexed 32QAM transmission over 60 km few-mode fiber. *Opt. Express* **2014**, *22*, 749–755. [CrossRef] [PubMed]
8. Ip, E. Gain Equalization for Few-Mode Fiber Amplifiers Beyond Two Propagating Mode Groups. *IEEE Photonics Technol. Lett.* **2012**, *24*, 1933–1936. [CrossRef]
9. Bairagi, R.N.; Roy, A.; Pervin, S.; Sher, S.M. Design of a Concentric Triple-core based Dispersion Compensating Fiber. In Proceedings of the 2019 4th International Conference on Electrical Information and Communication Technology (EICT), Khulna, Bangladesh, 20–22 December 2019.
10. Gaur, A.; Rastogi, V. Modal gain equalization of 18 modes using a single-trench ring-core EDFA. *J. Opt. Soc. Am. B* **2018**, *35*, 2211–2216. [CrossRef]
11. Jin, C.; Ung, B.; Messaddeq, Y.; LaRochelle, S. Tailored modal gain in a multi-mode erbium-doped fiber amplifier based on engineered ring doping profiles. In Proceedings of the Photonics North 2013, Ottawa, ON, Canada, 3 July 2013; pp. 1–12.
12. Wada, M.; Sakamoto, T.; Aozasa, S.; Mori, T.; Yamamoto, T.; Hanzawa, N.; Yamamoto, F. L-band 2-LP mode EDFA with low modal dependent gain. In Proceedings of the 2015 Optical Fiber Communications Conference and Exhibition (OFC), Los Angeles, CA, USA, 22–26 March 2015.
13. Jung, Y.; Kang, Q.; Sleiffer, V.A.; Inan, B.; Kuschnerov, M.; Veljanovski, V.; Corbett, B.; Winfield, R.; Li, Z.; Teh, P.S.; et al. Three mode Er3+ ring-doped fiber amplifier for mode-division multiplexed transmission. *Opt. Express* **2013**, *21*, 10383–10392. [CrossRef] [PubMed]
14. Jung, Y.; Alam, S.; Li, Z.; Dhar, A.; Giles, D.; Giles, I.P.; Sahu, J.K.; Poletti, F.; Grüner-Nielsen, L.; Richardson, D.J. First demonstration and detailed characterization of a multimode amplifier for space division multiplexed transmission systems. *Opt. Express* **2011**, *19*, B952–B957. [CrossRef] [PubMed]
15. Kang, Q.; Gregg, P.; Jung, Y.; Lim, E.L.; Alam, S.U.; Ramachandran, S.; Richardson, D.J. Amplification of 12 OAM Modes in an air-core erbium doped fiber. *Opt. Express* **2015**, *23*, 28341–28348. [CrossRef] [PubMed]
16. Bai, N.; Wang, T.; Li, G. Multimode fiber amplifier with tunable modal gain using a reconfigurable multimode pump. *Opt. Express* **2011**, *19*, 16601–16611. [CrossRef] [PubMed]

17. Kasahara, M.; Saitoh, K.; Sakamoto, T.; Hanzawa, N.; Matsui, T.; Tsujikawa, K.; Yamamoto, F. Design of Three-Spatial-Mode Ring-Core Fiber. *J. Lightwave Technol.* **2014**, *32*, 1337–1343. [CrossRef]
18. Yung, Y.; Alam, S.; Li, Z.; Dhar, A.; Giles, D.; Giles, I.; Sahu, J.; Grűner-Nielsen, L.; Poletti, F.; Richardson, D.J. First demonstration of multimode amplifier for spatial division multiplexed transmission systems. In Proceedings of the 37th European Conference and Exposition on Optical Communications, Geneva, Switzerland, 18 September 2011; p. Th.13.K.14.
19. Ono, H.; Hosokawa, T.; Ichii, K.; Matsuo, S.; Nasu, H.; Yamada, M. 2-LP mode few-mode fiber amplifier employing ring-core erbium-doped fiber. *Opt. Express* **2015**, *23*, 27405–27418. [CrossRef] [PubMed]
20. Jung, Y.; Kang, Q.; Shen, L.; Chen, S.; Wang, H.; Yang, Y.; Shi, K.; Thomsen, B.C.; Correa, R.A.; Eznaveh, Z.S.; et al. Few Mode Ring-Core Fibre Amplifier for Low Differential Modal Gain. In Proceedings of the 2017 European Conference on Optical Communication (ECOC), Gothenburg, Sweden, 17–21 September 2017; pp. 1–3.
21. Gregg, P.; Kristensen, P.; Ramachandran, S. Conservation of orbital angular momentum in air-core optical fibers. *Optica* **2015**, *2*, 267–271. [CrossRef]
22. Ye, J.; Li, Y.; Han, Y.; Deng, D.; Guo, Z.; Gao, J.; Sun, Q.; Liu, Y.; Qu, S. Excitation and separation of vortex modes in twisted air-core fiber. *Opt. Express* **2016**, *24*, 8310–8316. [CrossRef] [PubMed]
23. Gregg, P.; Kristensen, P.; Golowich, S.E.; Olsen, J.Ø.; Steinvurzel, P.; Ramachandran, S. Stable Transmission of 12 OAM States in Air-Core Fiber. In Proceedings of the CLEO: Science and Innovations 2013, San Jose, CA, USA, 9–14 June 2013; p. CTu2K.2.
24. Yamashita, Y.; Matsui, T.; Wada, M.; Aozasa, S.; Sakamoto, T.; Nakajima, K. Differential Modal Gain Reduction using a Void Inscribed in a Two-Mode-Erbium Doped Fiber. In Proceedings of the Optical Fiber Communication Conference 2020, San Diego, CA, USA, 8–12 March 2020; p. W4B.6.
25. Jung, Y.; Kang, Q.; Sidharthan, R.; Ho, D.; Yoo, S.; Gregg, P.; Ramachandran, S.; Alam, S.-U.; Richardson, D.J. Optical Orbital Angular Momentum Amplifier Based on an Air-Hole Erbium-Doped Fiber. *J. Lightwave Technol.* **2017**, *35*, 430–436. [CrossRef]
26. Krummrich, P.M.; Akhtari, S. Selection of energy optimized pump concepts for multi core and multi mode erbium doped fiber amplifiers. *Opt. Express* **2014**, *22*, 30267–30280. [CrossRef] [PubMed]
27. Kang, Q.; Lim, E.L.; Jung, F.P.; Baskiotis, C.; Alam, S.U.; Richardson, D.J. Minimizing differential modal gain in cladding-pumped EDFAs supporting four and six mode groups. *Opt. Express* **2014**, *22*, 21499–21507. [CrossRef] [PubMed]
28. Kang, Q.; Lim, E.-L.; Poletti, F.; Jung, Y.; Alam, S.-u.; Richardson, D.J. Minimizing Differential Modal Gain in Cladding Pumped MM-EDFAs for Mode Division Multiplexing in C and L Bands. In Proceedings of the International Photonics and OptoElectronics Meetings, Wuhan, China, 18–21 June 2014; p. FTh4F.1.
29. Chang, J.H.; Corsi, A.; Rusch, L.A.; LaRochelle, S. Design Analysis of OAM Fibers Using Particle Swarm Optimization Algorithm. *J. Lightwave Technol.* **2020**, *38*, 846–856. [CrossRef]
30. Le Cocq, G.; Quiquempois, Y.; Bigot, L. Optimization Algorithm Applied to the Design of Few-Mode Erbium Doped Fiber Amplifier for Modal and Spectral Gain Equalization. *J. Lightwave Technol.* **2015**, *33*, 100–108. [CrossRef]
31. Chu, T.; Wang, P.; Zhu, C. Modeling of Active Fiber Loop Ring-Down Spectroscopy Considering Gain Saturation Behavior of EDFA. *J. Lightwave Technol.* **2020**, *38*, 966–973. [CrossRef]